

Rheology of nanocomposites

Modelling and interpretation of nanofiller influence

Christophe Block · Nick Watzeels · Hubert Rahier ·
Bruno Van Mele · Guy Van Assche

ESTAC2010 Conference Special Issue
© Akadémiai Kiadó, Budapest, Hungary 2011

Abstract In this study, a methodology is developed for the quantitative characterisation of the nanofiller network in polymer nanocomposites via dynamic rheometry. Nanoclay-reinforced poly(ϵ -caprolactone) (PCL) nanocomposites were prepared by melt mixing. Frequency sweep experiments in the melt state display at low frequencies a solid-like elastic response that can be attributed to the formation of a physical nanofiller network. Combining a semi empirical model and the time–temperature superposition principle permits a reliable determination of the zero shear modulus that characterises the solid-like response of nanocomposites at low frequency, and which is related to the nanofiller dispersion.

Keywords Rheology · Nanocomposites · Solid-like behaviour · Model · Time–temperature superposition

Introduction

Improving material properties and creating more specific tailored properties have become more important over the last decades. Combining different materials to benefit from the usually very different properties creates better materials with the envisaged properties. Composite materials have been around for ages and have already proved their use. In recent years an increasing interest is shown in

nanocomposites. By choosing fillers with at least one dimension in the nanometre range, the surface to volume ratio increases tremendously. Thus, the interface between filler and matrix material increases, enabling a bigger impact of the filler properties on the overall properties, such as higher stiffness [1–3], higher melt strength, lower permittivity, and improved barrier properties [2, 4].

Due to the positive influence of these nanofillers in the nanocomposites, an abundance of articles on different methods to quantify the influence of the nanofiller can be found in literature. Many articles on assessing the clay dispersion in a polymer matrix by morphological [1, 5, 6] and rheological [5, 7, 8] studies have been published. Due to the relatively easy sample preparation and sample loading, rheology is often used to screen or characterise the nanofiller dispersion, or more generally the influence of the nanofiller on the overall rheological behaviour of (thermoplastic) nanocomposites. It is widely accepted that the melt strength increases with increasing nanoclay loading. This has been attributed to (pseudo) solid-like behaviour [1, 8–11], related to the physical network formation of the nanofiller [1, 3, 8, 10, 11]. Methods to quantify this behaviour include different representations, such as Cole–Cole plots [1, 7, 8, 12], where the imaginary part of the complex viscosity is plotted against the real part, and Van Gurp–Palmen plots [12, 13], where the loss angle is plotted as a function of the modulus of the nanocomposite. Representations as Cole–Cole and Van Gurp–Palmen plots emphasize or highlight the influence of the nanofiller; however, they tend not to characterise it. Some models are proposed in literature to quantify the influence of nanofiller on the overall rheology, such as shear-thinning exponent analysis [14], where the slope of the complex viscosity versus the frequency is the parameter that determines the dispersion quality.

C. Block · N. Watzeels · H. Rahier · B. Van Mele ·
G. Van Assche (✉)

Department of Physical Chemistry and Polymer Science
(FYSC), Vrije Universiteit Brussel (VUB), Pleinlaan 2,
B-1050 Brussels, Belgium
e-mail: gvassche@vub.ac.be

The evolution of the modulus of the absolute viscosity $|\eta^*|$ as a function of the angular frequency ω for nanocomposites can be described by Eq. 1 [15, 16]. This equation combines the Yasuda–Carreau equation [13, 15, 17] for describing the shear-thinning behaviour in shear experiments, with an additional term incorporating the influence of the nanofiller.

$$|\eta^*| = \frac{\sigma_0}{\omega} + \eta_0(1 + (\lambda\omega)^a)^{\frac{m-1}{a}} \quad (1)$$

The second term originating from Yasuda–Carreau [13, 15, 17] describes the first Newtonian plateau (given by the zero shear viscosity η_0) and the “shear-thinning” behaviour of the polymer matrix, with λ the relaxation time constant, a the Yasuda parameter, and m the dimensionless power law index. The first term, introduced in [15] as a “yield stress” contribution, was shown to be correlated with the degree of exfoliation of the nanofiller [16].

In this study, we prefer to describe the solid-like behaviour observed in dynamic rheometry experiments at low frequencies using a zero shear modulus G_0 , which represents the plateau modulus to which the absolute shear modulus evolves at low frequency, thus replacing σ_0 in Eq. 1 by G_0 (Eq. 2),

$$|\eta^*| = \frac{G_0}{\omega} + \eta_0(1 + (\lambda\omega)^a)^{\frac{m-1}{a}} \quad \text{with } G_0 = \lim_{\omega \rightarrow 0} |G^*| \quad (2)$$

In nanocomposites, the zero shear modulus G_0 characterises the solid-like behaviour at low frequency originating from the elastic contribution of the filler (network) to the overall rheological behaviour of the nanocomposite at low frequency. In frequency sweep experiments, lower angular frequencies will generally emphasize the solid-like behaviour of the nanofiller network (the first term in Eq. 2), whilst higher angular frequencies will emphasize the matrix contribution (the second term in Eq. 2).

The build up of this physical nanofiller network is not instantaneous, a certain time is needed depending on the viscosity of the polymeric matrix material, and it can be broken down upon shear [3, 10, 11]. In this study, we are not focussing nor trying to quantify this transient behaviour. Rather, by applying sufficiently long waiting times and small oscillation strains, a steady state response is measured.

Although Eq. 1 proved to be a useful tool to characterise the extent of exfoliation in nanocomposites [16], the limited extent of the frequency range accessible in a single rheological experiment often hampers a reliable determination of the fitting parameter σ_0 (or the equivalent G_0 in Eq. 2). In rheological simple fluids, thus systems with a single main relaxation time, the time–temperature superposition (TTS) principle can be applied to extend the range

of frequencies over which the rheological behaviour is determined (e.g. [18]). In this article, TTS is used to extend the frequency range accessible to dynamic rheometry for the study of nanocomposites, permitting a more reliable determination of the zero shear modulus G_0 in a straightforward methodology, and resulting in a quantitative measure of the solid-like behaviour of the nanofiller network observed at low frequencies.

Experimental

Materials

Poly(ε -caprolactone) (PCL) was obtained from Solvay Caprolactones (presently Perstorp Caprolactones, UK) and is commercialized under the trade name CAPA®6500 ($M_n = 47.500 \text{ g mol}^{-1}$ and $M_w = 84.500 \text{ g mol}^{-1}$, according to the manufacturer).

Cloisite®30B (in short C30B) is based on natural montmorillonite, exchanged with benzyl methyl bis(2-hydroxyethyl) tallowalkyl ammonium (Southern Clay Products, USA).

Nanocomposite preparation

The nanocomposites of this study, with filler contents up to 10 wt%, were prepared by melt mixing at 130 °C using a batch-operated lab-scale twin-screw DSM Xplore Micro-Compounder (15 cc, N₂ purge, screw rotation speed of 170 rpm). Unless otherwise specified, the residence time within the mixer was 30 min. All compositions are expressed in terms of the inorganic filler content, as determined from thermogravimetric analysis under nitrogen (TA Instruments Q5000 TGA, 25 mL min⁻¹ N₂).

Subsequent to melt mixing, all nanocomposites were compression-moulded at 140 °C under 100 bar pressure using an Agila PE 30 hydraulic press.

Characterisation techniques

Small angle oscillatory shear rheometry, also called dynamic rheometry, experiments were performed on a TA Instruments AR-G2 rheometer fitted with Electrically Heated Plates and using a 25 mm stainless steel cone-and-plate geometry (cone angle 4°). The linear viscoelastic region was determined from strain sweep experiments at a frequency of 1 Hz. After a resting time of 15 min, a frequency sweep, from 0.01 to 100 Hz, was conducted using a 1% strain. This resting time ensured a complete build up of the nanofiller network. Equivalent rheological curves are obtained for measurements having longer resting times (on the same sample) and for different samples of the same

nanocomposite. For extending the frequency range through the TTS principle, experiments were conducted at different temperatures.

Results and discussion

Figure 1 depicts two equivalent representations of a series of rheological experiments for C30B-filled PCL nanocomposites with loadings from 0 to 10 wt%, as well as the curves obtained by fitting Eq. 2. In Fig. 1 (top), the rheological data are depicted by the absolute viscosity $|\eta^*|$ as a function of the angular frequency ω . As already well established in literature, an increasing clay loading results in a more dominant solid-like behaviour in the low frequency range [1, 8–11]. This solid-like behaviour at low frequencies is better visualized in the representation shown in Fig. 1 (bottom), showing the absolute shear modulus $|G^*|$ versus ω . As the complex viscosity η^* is equal to the complex shear modulus divided by ω , Eq. 2 can be rewritten as:

$$|G^*| = G_0 + \eta_0 \cdot \omega (1 + (\lambda\omega)^a)^{\frac{m-1}{a}} \quad (3)$$

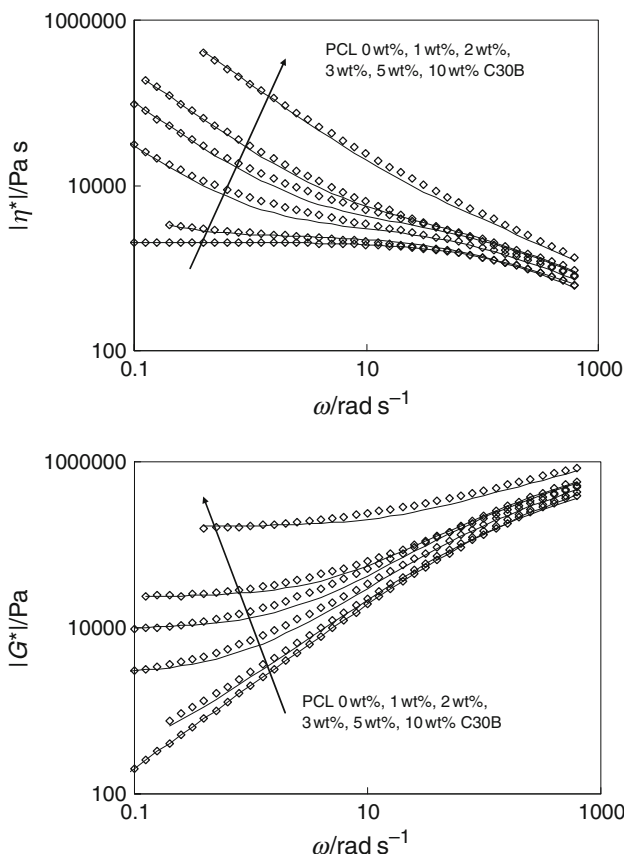


Fig. 1 Rheological data for PCL-C30B nanocomposites with different loadings measured at 100 °C (symbols), depicted together with the fitted G_0 corrected Yasuda–Carreau model of Table 1

Fitting either Eqs. 2 or 3 to the corresponding data sets gave the same results.

The model used can be seen as a two-phase model, containing one contribution representing the matrix and one representing the filler network. When increasing the loading of this particular nanoclay from 1 to 10 wt%, the zero shear modulus G_0 obtained from fitting increases over three orders of magnitude (Table 1). This makes G_0 appropriate to quantify via a single parameter the solid-like behaviour of the nanofiller network. Adding well-dispersed nanofiller to the matrix is also likely to alter the rheological behaviour of the polymer close to the filler particles due to matrix–particle interactions. In Table 1, the influence of the nanofiller on the matrix material can be found in the changing of the Newtonian plateau viscosity η_0 and relaxation time constant λ . Although the model agrees fairly well with the experimental data over the frequency range depicted, a somewhat poorer agreement is observed between 1 and 10 rad s⁻¹, around the transition from the solid-like behaviour at lower frequencies to the matrix-dominated behaviour at higher frequencies. This indicates that more complex models would be required to account for the detailed rheological behaviour of the nanocomposites. Nevertheless, since the characterisation of the filler network through its solid-like behaviour is mainly focusing on the low frequency range, when the contribution of the nanofiller network dominates the matrix contribution, the parameter G_0 can be well quantified if data are available over a frequency range sufficiently extended to the low frequency region.

It is worth noting that in case the first Newtonian plateau (parameterized by η_0) is too high, the low frequency solid-like behaviour may not be detected in the frequency range chosen for that particular experiment, making the determination of the parameter G_0 impossible. On the other hand, the solid-like behaviour of the nanofiller can dominate the rheological behaviour of the nanocomposite over the full frequency range, e.g. at high loading, thus hampering the reliable determination of the parameters

Table 1 Parameters of the fittings of the G_0 corrected model (Eqs. 2 and 3) on the rheological data for pure PCL CAPA 6500 and C30B nanocomposites 1 to 10 wt% shown in Fig. 1

	PCL	1 wt%	2 wt%	3 wt%	5 wt%	10 wt%
G_0/Pa^a	0	172	2733	9724	23288	165906
$\eta_0/\text{Pa s}^a$	2042	2407	3000	3600	3600	4000
λ/s	0.0095	0.0154 ^b	b	b	b	b
m	0.408 ^c	c	c	c	c	c
a	0.949 ^c	c	c	c	c	c

Note: ^a G_0 and η_0 were optimized individually for each sample

^b Taken same for all filler loadings

^c Taken same as for pure PCL

describing the rheological behaviour of the polymer matrix (the second term in Eq. 2).

Considering the previous remarks, in order to quantify the elastic response of the nanofiller network, extending the data to the low frequency region is advisable, thus decreasing the influence of the polymer matrix in the rheological data. Alternatively, by increasing the temperature, the influence of the polymer matrix can be decreased by decreasing the viscosity η_0 . Thus, applying the TTS principle extending the frequency range to lower frequency, highlighting the filler contribution. On the other hand, lowering the temperature makes the matrix contribution of the polymer more dominant, thus enabling a better estimation of the Yasuda–Carreau parameters of the second term in Eqs. 2 and 3.

The extension of the frequency range by TTS is achieved by shifting the rheological information retrieved at other temperatures to a reference temperature. The shift factor a_T is the horizontal shift of the frequency to superpose the absolute shear modulus curve $|G^*(\omega, T)|$ at a given temperature T onto the absolute shear modulus curve $|G^*(\omega, T_{ref})|$ measured at the reference temperature T_{ref} [18].

$$\log(a_T) = \log(\omega_{ref}) - \log(\omega) = \log\left(\frac{\omega_{ref}}{\omega}\right) \quad (4)$$

with

$$|G^*(\omega, T)| = |G^*(\omega, T_{ref})| \quad (5)$$

In this way, a master curve $|G^*(\omega, T_{ref})|$ is created at the reference temperature.

TTS can also be applied on absolute viscosity $|\eta^*|$ curves, which will need a horizontal and a vertical shift with the same shift factor a_T :

$$|\eta^*(\omega, T)| = \frac{|G^*(\omega, T)|}{\omega} = \frac{|G^*(\omega, T_{ref})|}{\omega_{ref}/a_T} = a_T \cdot |\eta^*(\omega, T_{ref})| \quad (6)$$

In other words, to superpose absolute viscosity data $|\eta^*(\omega, T)|$ at a temperature T on the absolute viscosity curve $|\eta^*(\omega, T_{ref})|$ at the reference temperature, $|\eta^*(\omega, T)|$ needs to be divided by the same shift factor a_T as the one multiplied with the angular frequency ω . This is illustrated in Fig. 2 for pure PCL, where the shift of experimental data measured at 70 and 160 °C to the master curve at a reference temperature of 100 °C is illustrated. The master curve obtained by TTS is shown in Fig. 3. Note in Fig. 3 how the experimental data at T_{ref} (100 °C) are extended towards higher and lower frequencies by means of measurements at lower and higher temperature, respectively, as indicated with the arrows. Higher temperatures lower the viscosity and shift the onset of the “shear-thinning” region to higher frequencies and vice versa.

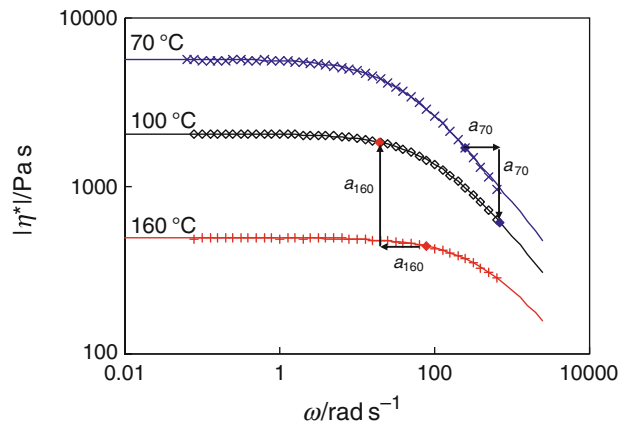


Fig. 2 Rheological data (symbols) of pure PCL at 70 °C (times symbol), 100 °C (diamond), and 160 °C (plus sign) together with the fitted model with parameters of Table 2. The arrows indicate how the data shift horizontally and vertically to construct a master curve at $T_{ref} = 100$ °C (see Fig. 3)

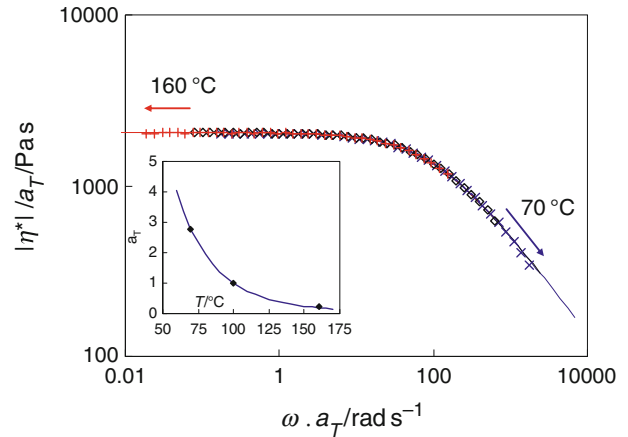


Fig. 3 Master curve obtained by applying time–temperature superposition for pure PCL. The data from Fig. 2 were shifted to superpose on the rheological data at $T_{ref} = 100$ °C and are plotted together with the fitted model (lines) using the parameters of Table 2. The inserted graph shows the WLF temperature dependency of the shift factor

In relation to the modelling of the rheological data, it should be noted that the relaxation time constant λ in Eqs. 1–3 is also temperature dependent: λ represents the inverse of the angular frequency at the onset of shear thinning and should be shifted in the same way as the viscosity (Eq. 7):

$$\lambda_{ref} = \frac{\lambda}{a_T} \quad (7)$$

So the angular frequency ω , the Newtonian plateau value of the viscosity η_0 , and the relaxation time constant λ need to be modified with the shift factor a_T . In contrast, the modelling parameter G_0 is assumed to be temperature independent over the limited temperature range evaluated

Table 2 Parameters of the fittings of the Yasuda–Carreau model (second term in Eqs. 2 and 3) on the rheological data for pure PCL given in Figs. 2 and 3

T/°C	a_T	G_0/Pa	$\eta_0/\text{Pa s}$	λ/s	m	a
70	2.78	^a	$a_{70} \cdot \eta_0(T_{\text{ref}})$	$a_{70} \cdot \lambda(T_{\text{ref}})$	^a	^a
100	1	0^{a}	2042 ^a	0.0095 ^a	0.408 ^a	0.949 ^a
160	0.24	^a	$a_{160} \cdot \eta_0(T_{\text{ref}})$	$a_{160} \cdot \lambda(T_{\text{ref}})$	^a	^a

Note: ^aTaken same as in table 1

for the TTS procedure, in agreement with the experiments. In Table 2, the model parameters for the fittings of the data in Figs. 2 and 3 are given.

Figure 4 shows the influence of temperature on the rheological behaviour of a PCL nanocomposite containing 3 wt% C30B. As the temperature is raised, the contribution of the polymer matrix decreases. Due to the decrease of the viscosity of the first Newtonian plateau (η_0 in Eqs. 2 and 3) with temperature, the solid-like behaviour of the nanofiller network is dominating the rheological response of the nanocomposite up to higher frequencies. Generally

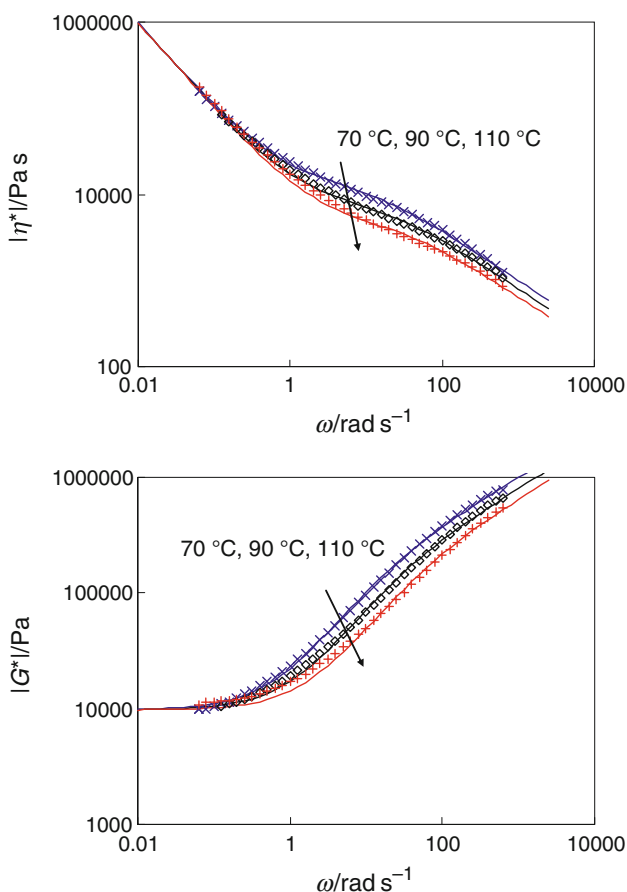


Fig. 4 PCL nanocomposite containing 3 wt% C30B; rheological data (symbols) at 70 °C (times symbol), 90 °C (diamond), and 110 °C (plus sign) are plotted together with the fitted model (lines)

speaking, measurements at higher temperatures can be used to confirm the presence of low frequency solid-like behaviour resulting from nanofiller networks.

Figure 5 confirms that the TTS principle also applies to the nanocomposites, as was already reported by other researchers [8–10, 19, 20]. From the view point of the modelling, this requires that the parameter G_0 is quasi or completely temperature independent, as confirmed by the superposition of the solid-like behaviour in the low frequency region (Fig. 4 and Table 3). Compared to the temperature dependency of the rheology of the polymer matrix (seen in the mid-frequency region), no noticeable variation is observed in G_0 . Taking into account that the measurements were performed on different samples and that G_0 changes by three orders of magnitude going from 1 to 10 wt% filler, the non-perfect overlap of the experimental data obtained at different temperatures after shifting to the master curve can be safely neglected. The parameters obtained by fitting the experimental data in Figs. 4 and 5 are given in Table 3.

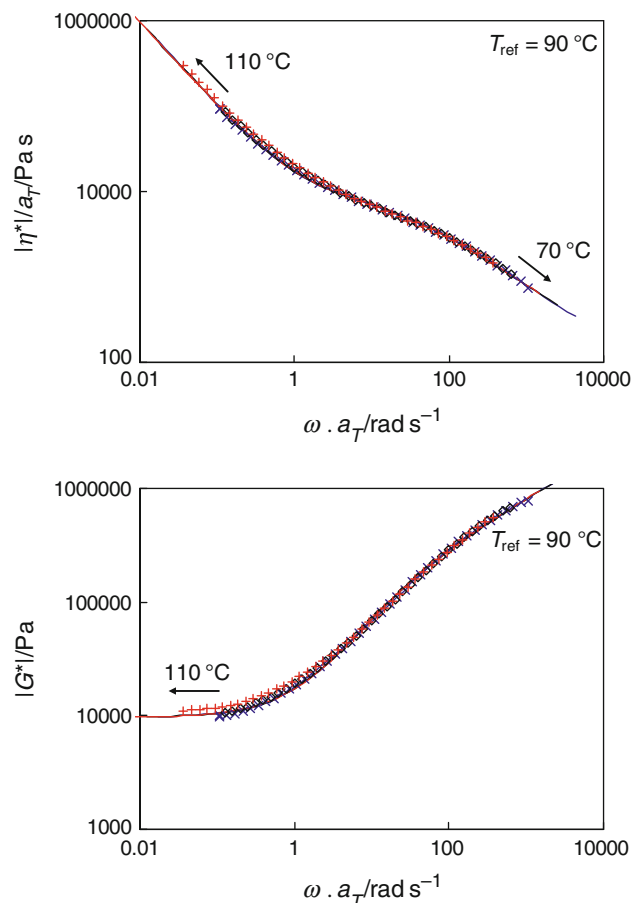


Fig. 5 Master curve obtained by applying time-temperature superposition for a PCL nanocomposite containing 3 wt% C30B. The data from Fig. 4 were shifted to superpose on the rheological data at $T_{\text{ref}} = 90$ °C and are plotted together with the fitted model (lines)

Table 3 Parameters of the fittings of the G_0 corrected model (Eqs. 2 and 3) on the rheological data for PCL + 3 wt% C30B shown in Figs. 4 and 5

T/°C	a_T	G_0/Pa	$\eta_0/\text{Pa s}$	λ/s	m	a
70	1.7	^c	$a_{70} \cdot \eta_0(T_{\text{ref}})$	$a_{70} \cdot \lambda(T_{\text{ref}})$	^a	^a
90	1	9979 ^b	7759 ^b	0.0457 ^b	0.408 ^a	0.949 ^a
110	0.59	^c	$a_{110} \cdot \eta_0(T_{\text{ref}})$	$a_{110} \cdot \lambda(T_{\text{ref}})$	^a	^a

Note: ^aTaken same as in Table 1

^b Different values as Table 1 since this is a different sample, however, only 2.5% variation

^c Taken same as $T_{\text{ref}} = 90^\circ \text{C}$

Time–temperature superposition enlarges the experimental frequency range, as illustrated in Fig. 5 with the arrows, permitting a better estimation of the fitting parameters of the extended Yasuda–Carreau model, including the zero shear modulus G_0 that is characteristic for the nanofiller network.

Conclusions

Studying the rheological behaviour of nanocomposites by dynamic rheometry offers a mechanical approach for the detection of the nanofiller network. If the nanofiller particles form a physical, percolating network, a solid-like behaviour is observed at low frequencies in case the viscosity of the polymer matrix is low enough. At higher temperatures (in the melt state of the polymer matrix) or lower frequencies, the characteristics of the nanofiller network are highlighted.

The combination of the zero shear modulus G_0 corrected Yasuda–Carreau model with the extension of the frequency range by TTS permits the determination of G_0 , which represents the elastic contribution of the filler network. G_0 proves to be temperature independent within the error of the experiments and modelling, and within the temperature range studied. TTS extends the frequency range and thus enables a more rigorous investigation of the low frequency region, where the nanofiller network influence is best quantified. This straightforward methodology is currently used to study the influence of organomodifiers and processing conditions on the rheological behaviour of nano-clay-reinforced nanocomposites.

Acknowledgements This study is supported by the agency for Innovation by Science and Technology (IWT-Flanders, Belgium), the Research Foundation-Flanders (FWO, Belgium), and TA Instruments (Delaware, USA).

References

- Qualitative assessment of nanofiller dispersion in poly(e-caprolactone) nanocomposites by mechanical testing, dynamic rheometry and advanced thermal analysis. *Eur Polym J.* 2010;46:984–96.
2. Alexandre M, Dubois P. Polymer-layered silicate nanocomposites: preparation, properties and uses of a new class of materials. *Mat Sci Eng R.* 2000;28:1–63.
 3. Solomon MJ, Almusallam AS, Seefeldt KF, Somwangthanaroj A, Varadhan P. Rheology of polypropylene/clay hybrid materials. *Macromolecules.* 2001;34:1864–72.
 4. LeBaron PC, Wang Z, Pinnavaia T. Polymer-layered silicate nanocomposites: an overview. *J Appl Clay Sci.* 1999;15:11–29.
 5. Potschke P, Fornes TD, Paul DR. Rheological behavior of multiwalled carbon nanotube/polycarbonate composites. *Polymer.* 2002;43(11):3247–55.
 6. Gelfer MY, Song HH, Liu LZ, Hsiao BS, Chu B, Rafailovich M, Si MY, Zaitsev V. Effects of organoclays on morphology and thermal and rheological properties of polystyrene and poly(methyl methacrylate) blends. *J Polym Sci Polym Phys.* 2003;41:44–54.
 7. Szazdi L, Abranyi A, Pukanszky BJ, Vancso JG, Pukanszky B. Morphology characterization of PP/clay nanocomposites across the length scales of the structural architecture. *Macromol Mater Eng.* 2006;291:858–68.
 8. Wu D, Wu L, Sun Y, Zhang M. Rheological properties and crystallization behavior of multi-walled carbon nanotube/poly(e-caprolactone) composites. *J Polym Sci Polym Phys.* 2007;45:3137–47.
 9. Krishnamoorti R, Giannelis EP. Rheology of end-tethered polymer layered silicate nanocomposites. *Macromolecules.* 1997;30:4097–102.
 10. Cassagnau P. Melt rheology of organoclay and fumed silica nanocomposites. *Polymer.* 2008;49:2183–96.
 11. Vermant J, Ceccia S, Dolgovskij MK, Maffettone PL, Macosko CW. Quantifying dispersion of layered nanocomposites via melt rheology. *J Rheol.* 2007;51:429–50.
 12. Wu D, Wu L, Zhang M. Rheology of multi-walled carbon nanotube/poly(butylene terephthalate) composites. *J Polym Sci Polym Phys.* 2007;45:2239–51.
 13. Wang B, Sun G, He X, Liu J. The Effect of multiwall carbon nanotube on the crystallization, morphology, and rheological properties of Nylon1010 nanocomposites. *J Polym Eng Sci.* 2007;47:1610–20.
 14. Wagener R, Reisinger TJG. A rheological method to compare the degree of exfoliation of nanocomposites. *Polymer.* 2003;44(24):7513–8.
 15. Berzin F, Vergnes B, Delmare L. Rheological behavior of controlled-rheology polypropylenes obtained by peroxide-promoted degradation during extrusion: comparison between homopolymer and copolymer. *J Appl Polym Sci.* 2001;80:1243–52.
 16. Lertwilarmun W, Vergnes B. Influence of compatibilizer and processing conditions on the dispersion of nanoclay in a polypropylene matrix. *Polymer.* 2005;46:3462–71.
 17. Yasuda K, Armstrong RC, Cohen RE. Shear flow properties of concentrated solutions of linear and star branched polystyrenes. *Rheol Acta.* 1981;20:163–78.
 18. Young RJ, Lovell PA. Introduction to polymers. 2nd ed. Boca Raton: CRC Press LLC; 1991.
 19. Zhao J, Morgan AB, Harris JD. Rheological characterization of polystyrene–clay nanocomposites to compare the degree of exfoliation and dispersion. *Polymer.* 2005;46:8641–60.
 20. Krishnamoorti R, Ren J, Silva AS. Shear response of layered silicate nanocomposites. *J Chem Phys.* 2001;114(11):4968–73.